Biomedicine & Pharmacotherapy 178 (2024) 117191

Contents lists available at ScienceDirect

Biomedicine & Pharmacotherapy

journal homepage: www.elsevier.com/locate/biopha

Pharmacological inhibition of CK2 by silmitasertib mitigates sepsis-induced circulatory collapse, thus improving septic outcomes in mice

Gustavo Ferreira Alves [a,b,c], Eleonora Aimaretti [d], Maria Luísa da Silveira Hahmeyer [b], Giacomo Einaudi [c], Elisa Porchietto [c], Chiara Rubeo [d], Enrica Marzani [a], Manuela Aragno [d], José Eduardo da Silva-Santos [b], Carlo Cifani [c], Daniel Fernandes [b,1], Massimo Collino [a,*,1]

[a] Department of Neurosciences (Rita Levi Montalcini), University of Turin, Turin, Italy
[b] Department of Pharmacology, Federal University of Santa Catarina, Florianópolis, Brazil
[c] Pharmacology Unit, School of Pharmacy, University of Camerino, Camerino, Italy
[d] Department of Clinical and Biological Sciences, University of Turin, Turin, Italy

ARTICLE INFO

Keywords:
Septic shock
Casein Kinase-2
Nitric oxide
Inflammation
Vasoplegia
CX-4945

ABSTRACT

Casein kinase II (CK2) has recently emerged as a pivotal mediator in the propagation of inflammation across various diseases. Nevertheless, its role in the pathogenesis of sepsis remains unexplored. Here, we investigated the involvement of CK2 in sepsis progression and the potential beneficial effects of silmitasertib, a selective and potent CK2α inhibitor, currently under clinical trials for COVID-19 and cancer. Sepsis was induced by caecal ligation and puncture (CLP) in four-month-old C57BL/6OlaHsd mice. One hour after the CLP/Sham procedure, animals were assigned to receive silmitasertib (50 mg/kg/i.v.) or vehicle. Plasma/organs were collected at 24 h for analysis. A second set of experiments was performed for survival rate over 120 h. Septic mice developed multiorgan failure, including renal dysfunction due to hypoperfusion (reduced renal blood flow) and increased plasma levels of creatinine. Renal derangements were associated with local overactivation of CK2, and downstream activation of the NF-κB-iNOS-NO axis, paralleled by a systemic cytokine storm. Interestingly, all markers of injury/inflammation were mitigated following silmitasertib administration. Additionally, when compared to sham-operated mice, sepsis led to vascular hyporesponsiveness due to an aberrant systemic and local release of NO. Silmitasertib restored sepsis-induced vascular abnormalities. Overall, these pharmacological effects of silmitasertib significantly reduced sepsis mortality. Our findings reveal, for the first time, the potential benefits of a selective and potent CK2 inhibitor to counteract sepsis-induced hyperinflammatory storm, vasoplegia, and ultimately prolonging the survival of septic mice, thus suggesting a pivotal role of CK2 in sepsis and silmitasertib as a novel powerful pharmacological tool for drug repurposing in sepsis.

1. Introduction

Sepsis and septic shock represent a major public health burden due to high morbidity and mortality rates, where 1 out of 5 deaths globally are associated with the disease [1]. Despite improvements in standard care, a significant mortality rate persists in sepsis, with an overall fatality rate of 25 %, escalating to a mortality rate of 40–50 % for cases of septic shock [2]. The current standard care includes controlling the infectious source, antibiotic therapy, haemodynamic supply, oxygen support and use of vasopressor drugs [3]. However, there remains a notable absence of selective therapies that could substantially improve sepsis outcomes.

Amidst the multifaceted responses elicited during the early stages of sepsis, vasoplegia emerges as a central circulatory component, potentially evoked, at least in part, by a hyper-inflammatory state. This phenomenon, in turn, leads to tissue hypoperfusion, thereby contributing to multiorgan failure and, ultimately, death [4,5]. Hence, pharmacological targeting of the disease's upstream determinants is imperative for retarding its progression and establishing successful prevention strategies. In light of this, we have recently demonstrated that targeting kinases constitutes a potent pharmacological approach for counteracting inflammatory disturbances in the septic context [6–8].

In recent years, significant attention has been directed towards

* Correspondence to: Department of Neurosciences (Rita Levi Montalcini), Corso Raffaello 30, Torino 10125, Italy.
E-mail address: massimo.collino@unito.it (M. Collino).
[1] These authors share senior authorship.

https://doi.org/10.1016/j.biopha.2024.117191
Received 27 May 2024; Received in revised form 12 July 2024; Accepted 22 July 2024
Available online 30 July 2024

casein kinase 2 (CK2), a highly conserved serine/threonine kinase, particularly in the realm of cancer research. CK2 comprises a tetrameric protein structure composed of two catalytic and two regulatory subunits. The catalytic subunits are encoded by two distinct genes, CSNK2A1 and CSNK2A2, denoted as α and α′, respectively. Conversely, the CK2 regulatory subunit, denoted as β, is encoded by the CSNK2B gene [9]. Under physiological conditions, CK2 phosphorylates a diverse array of substrates, numbering over 300, involved in governing several cellular processes, including DNA replication, gene transcription, signal transduction, cell growth, and apoptosis [10]. Nonetheless, aberrant CK2 activity has been well-documented across a spectrum of human cancers, where this dysregulated activity fosters a microenvironment conducive to neoplastic development, increasing cell proliferation and inhibiting apoptotic processes [11,12]. Within this paradigm, CK2 has additionally been implicated in perpetuating inflammatory cascades via various cellular pathways. Notably, CK2 activates key cytokine-associated downstream proteins, including Janus kinase (JAK) and signal transducer and activator of transcription (STAT), suggesting its role in the progression of inflammatory processes [13,14]. Consistently, it has been reported that CK2 can boost NF-κB's transcriptional activity by directly phosphorylating the IκBα subunits [15]. Intriguingly, as these pathways are well-documented to play a central role in the septic context, these findings strongly suggest that CK2 may potentially trigger detrimental responses in sepsis.

The pharmacological inhibition of CK2 represents a powerful pharmacological strategy that has demonstrated efficacy in mitigating inflammation and tissue damage in experimental models of rheumatoid arthritis [16] and renal ischemia/reperfusion [17]. Notably, an auspicious high selective CK2 inhibitor, named silmitasertib (previously reported as CX-4945) has raised significant attention due to its potent and dose-dependent antitumor effects in experimental models of prostate cancer [18] and glioblastoma [11]. Furthermore, silmitasertib has undergone evaluation in a variety of clinical trials aimed to target cancer as well as COVID-19 (clinicaltrials.gov; identifier codes: NCT00891280; NCT01199718; NCT02128282; NCT03904862; NCT03897036; NCT04663737; NCT04668209; NCT06202521; NCT05817708; NCT04668209). Here, we hypothesise that CK2 triggers deleterious responses in sepsis and, thus, the present study aims to explore the impact of its pharmacological inhibition by silmitasertib in a murine model of caecal ligation and puncture (CLP)-induced sepsis, assessing markers of multiorgan failure, inflammation and vascular abnormalities.

2. Material and methods

2.1. Animals

This study was carried out on 79 four-week-old, male C57BL/6 mice (30 from Envigo laboratories - Italy, and 49 from the Laboratory of Experimental Pharmacology at Federal University of Santa Catarina, Brazil). The mice, weighing between 30 and 35 g were housed under standard laboratory conditions, including *ad libitum* access to water and a standard chow diet. Housing arrangements included controlled temperature (25 ± 2 ºC) and a 12/12-hour light/dark cycle. Each cage was supplemented with environmental enrichment to accommodate five mice.

2.2. CLP-induced polymicrobial sepsis

Experimental sepsis was induced using the caecal ligation and puncture (CLP) model [21]. Briefly, mice were anesthetised in an anaesthetic chamber with isoflurane (IsoFlo, Abbott Laboratories, 3 L/min) and oxygen (1 L/min). Once sedated, anaesthesia was maintained during surgery with a ratio of isoflurane (2 L/min) and oxygen (1 L/min) delivered *via* nosecone. The abdominal surface of the mice was shaved and sterilised with 70 % alcohol. A longitudinal laparotomy (approximately 1 cm) was made along the *linea alba* using disposable scalpel blades to expose the caecum. The caecum was fully occluded just below the ileocaecal valve with a cotton thread, followed by a double puncture using a sterile needle (21 G). Gentle pressure was applied to the caecum to release small droplets of faecal content (approximately 2 mm). Subsequently, the caecum was carefully repositioned into its anatomical position, and the incision was sutured with a silk thread. Sham-operated mice underwent identical surgical procedures without CLP. Immediately after surgery, all mice received subcutaneous injections of 50 mL/kg of sterile resuscitation fluid (0,9 % NaCl at 37 °C), along with an analgesic agent (carprofen, 5 mg/kg, Pfizer, New York, New York, USA). Throughout the procedure, mice were maintained on a heated blanket at 37 °C and continuously monitored until they regained consciousness from anaesthesia.

2.3. Experimental design and treatment

Two *in vivo* experimental sets (a short-term follow-up and a survival study) were used in this study, and both followed the same treatment schedule. The animals were randomly allocated into three experimental groups, namely: Sham+Vehicle, CLP+Vehicle and CLP+Silm. One hour after surgery, mice were intravenously administered a single dose of either vehicle (phosphate-buffered saline, PBS, pH 7.4) or silmitasertib (Silm, 50 mg/kg, MedChemExpress, Princeton, New Jersey, USA). The chosen dose was defined based on previous *in vivo* studies [18,22].

2.4. Assessment of sepsis severity

Twenty-four hours after sepsis onset, an observational clinical score was applied by experienced blinded researchers to determine the health status of the animals. Six criteria were taken into consideration: piloerection, lethargy, periorbital exudates, respiratory distress, diarrhoea, and tremors. A clinical score exceeding 3 was designated as indicative of severe sepsis, whereas a score between 3 and 1 was characterised as moderate sepsis [6]. Mice's body temperature was also recorded at 24 h following sepsis insult.

2.5. In vivo assessment of renal blood flow (RBF)

At 24 h, following the assessment of sepsis severity, mice were deep anaesthetised with isoflurane, as previously described, and a longitudinal incision of ~1 cm was performed in the animals' left flank. Then, a laser probe (model VP1T) connected to the blood flow monitoring laser Doppler (moor VMS-LDF2, Moor Instruments, England) was carefully placed on the renal surface. The surgical incision was kept hydrated with gauze soaked with sterile PBS. RBF baseline data (in perfusion unit, PU) were recorded after 10 minutes of stabilisation.

2.6. Blood and organ collection

Biological samples were collected in a short-term follow-up study. Twenty-four hours after the surgical procedures, animals under deep anaesthesia (isoflurane) were prepared for blood withdrawn (~1.5 mL) by cardiac puncture, which was transferred to microtubes containing ethylenediaminetetraacetic acid (EDTA 5 %). Mice were then euthanised by cervical dislocation to collect the thoracic aorta artery and kidneys. Segments of the aortas were immediately used for *ex vivo* experiments in an organ bath system. The aorta, kidneys and plasma samples (obtained after centrifugation of whole blood, 1000 *g* at R.T.) were immediately frozen in liquid nitrogen and then stored at −80°C for subsequent molecular analysis.

2.7. Survival study

A long-term follow-up study was carried out to assess the pharmacological impact of silmitasertib on sepsis mortality. Twenty-eight mice underwent CLP-induced sepsis and were randomly assigned to two

experimental groups: one receiving vehicle and the other silmitasertib (50 mg/kg/i.v.), one-hour post-CLP (n = 14 per group). The survival status of mice in each group was evaluated every 12 hours over 120 hours (5 days).

2.8. Cytokine analysis

Pro- and anti-inflammatory cytokines were quantified in plasma samples by using the Luminex suspension coupled magnetic bead-based multiplexed Bio-Plex Pro™ Mouse Cytokine Th17 Panel A 6-Plex (#M6000007NY) assay (BioRad, Kabelsketal, Germany). The multiplex assay detects IL-1β, IL-6, TNF-α, IL-17, IFN-γ and IL-10 which were measured according to the manufacturer's instructions.

2.9. Biochemical analysis

Plasma samples were used to measure biomarkers of organ injury/dysfunction. Creatinine (#7075), urea (#7144), aspartate aminotransferase (AST) (#7036), alanine aminotransferase (ALT) (#7018), amylase (#7146) and lactate dehydrogenase (LDH) (#7096) were determined using commercially available clinical assay kits (FAR Diagnostics, Verona, Italy) following the manufacturer's instructions.

2.10. Kidney injury molecule-1 (KIM-1) analysis

KIM-1 was investigated in renal tissues. Kidney samples were snap frozen in liquid nitrogen using optimal cutting temperature (OCT) compound and stored at −80 °C freezer. Cryostat sections (10 μM) were obtained (Thermo Scientific HM525 NX, Thermo Fisher Scientific, Rockford, Illinois, USA). KIM-1 immunopositivity was analysed by immunohistochemistry. Slides were fixed (10 min) in acetone post-sectioning. Slides were then incubated over 2 h with primary antibody (the dilution 1:50, RT; #PA5–98302, Invitrogen, Waltham, Massachusetts, USA). Subsequently slices were incubated for 1 h with horseradish peroxidase (HRP)-conjugated secondary antibodies (dilution 1:200, RT, #7074). The chromogenic detection was obtained by adding 3,3'-diaminobenzidine (DAB) substrate and the nucleus was counterstained with hematoxylin.

2.11. qRT-PCR

Total RNA was extracted from kidney samples (~10 mg) using Total RNA Purification Kit (#37500, Norgen Biotek Corp, Ontario, Canada), following manufacturer's protocol. The concentration and purity of the RNA were assessed using the NanoDrop system (Thermo Fischer Scientific, Madison, Wisconsin, USA). Subsequently, 800 ng of total RNA was reverse-transcribed into complementary DNA (cDNA) using the SensiFAST™ cDNA Synthesis Kit 50 reactions (#BIO-65053 Meridian Bioscience, USA). Quantitative RT-PCR was performed using 100 ng of cDNA to evaluate the transcript levels of the target genes using SensiFAST™ SYBR® No-ROX Kit (#BIO-98005 Meridian Bioscience, USA). The reaction was carried out on the CFX Connect qRT-PCR Detection System (Bio-Rad Laboratories S.r.l., California, USA). Relative gene expression was normalised to the expression of the housekeeping gene 18 S and GAPDH. All samples were analysed in duplicate, and fold changes were determined by comparing them to the sham group using the formula ($2^{-\Delta\Delta CT}$) as previously described [23]. Primer sequences (Metabion international AG, Planegg, Germany) were the following: 18 S (Forward: TGC GAG TAC TCA ACA CCA ACA; Reverse: CTG CTT TCC TCA ACA CCA CA), GAPDH (Forward: TGA GCC TCC TCC AAT TCA ACC C; Reverse: CGG CCA AAT CCG TTC ACA CC), CSNK2α1 (Forward: ATG ACC ACC AGT CAC GGC TC; Reverse: CGA GCC TGG TCC TTC ACA AC).

2.12. Immunoblot analysis

Semi-quantitative western blot analysis was conducted on renal tissue samples. Approximately 50 mg of kidney samples were extracted, homogenised and subsequently centrifuged at 10,000 *g* for 25 min at 4 °C. Total protein content was determined using bicinchoninic acid (BCA) protein assay (Thermo Fisher Scientific, Rockford, Illinois, USA). Following quantification, proteins underwent electrophoretic separation using 8–10 % sodium dodecyl-sulfate polyacrylamide gel electrophoresis (SDS-PAGE) and subsequently transferred to polyvinylidene fluoride (PVDF) membranes. The membranes were then blocked using a 10 % milk solution with TBS-Tween and incubated overnight at 4 °C with the primary antibody. The primary antibodies and dilutions used were: 1:1000 rabbit anti-Tyr^{255} CK2α (#SAB4504299, Sigma, Darmstadt, Hessen, Germany); 1:1000 rabbit anti-total CSNK2α1 (#ab76040, Abcam, Cambridge, Cambridgeshire, United Kingdom); 1:1000 rabbit anti-$Ser^{176/180}$ IKKα/β (#2697 S); 1:1000 rabbit anti-total IKKβ (#2370 S); 1:1000 mouse anti- $Ser^{32/36}$ IκBα (#9246 S); 1:1000 mouse anti-total IκBα (#4814 S); 1:1000 rabbit anti-p50-NF-κB (#135865); 1:1000 rabbit anti-iNOS (#7271, Santa Cruz, Wembley, London, United Kingdom); 1:1000 mouse anti-NRLP3 (#A41812012, Adipogen, Füllinsdorf, Basel-Landschaft, Switzerland); 1:1000 rabbit anti-Caspase-1 (#24232 S); 1:1000 rabbit anti-IL-1β (#12242 S). Anti-mouse β-tubulin (#86298 S), anti-rabbit β-actin (#4970 S) and anti-rabbit GAPDH (#5174 S) were used as total or cytosolic housekeepings, while for nuclear loading control, anti-rabbit histone H3 (#4499 S). On the subsequent day, secondary antibodies (anti-mouse #7076; anti-rabbit #7074) conjugated with HRP at a dilution of 1:10,000 were applied and incubated for 60 min at room temperature. The membranes were washed with TBS-Tween and subjected to enhanced chemiluminescence substrates. Immunoreactive bands were assessed and semi-quantified using Bio-Rad Image Lab SoftwareTM 6.0.1 (Hercules, California, USA), and the results were normalised to the sham bands. Unless otherwise specified, antibodies were purchased from Cell Signaling Technology, Danvers, Massachusetts, USA.

2.13. Detection of tissue nitric oxide

Tissue samples (thoracic aortas and kidneys) were snap frozen in liquid nitrogen using OCT compound and stored at −80 °C freezer. Cryostat sections (aorta 5 μM, kidney 10 μM) were obtained and placed at poly-lysine (Sigma–Aldrich, Saint Louis, MO, USA) coated slides. The slides were divided into two groups: one to determine the tissue autofluorescence and the other to detect nitric oxide using the DAF-2 DA (diaminofluorescein-2 diacetate; Invitrogen, Waltham, MA, USA). Afterwards, the slides were incubated with Krebs-Ringer solution (concentrations, in mM: NaCl 130.0, KCl 4.7, KH_2PO_4 1.18, $MgSO_4$.7 H_2O 1.17, $NaHCO_3$ 14.9, D-glucose 5.5, $CaCl_2$.2 H_2O 1.6) at 37 °C for 30 minutes. Tissue sections were then incubated with diluted DAF-2 DA solution at 37 °C for 30 minutes. An additional incubation of 15 minutes with a fresh DAF-2 DA solution was made to ensure complete de-esterification of the diacetates. Then, the slides were washed with Krebs solution, and the nuclear labelling with DAPI (4,6-diamidino-2-phenylindole, 1 μg/mL, Thermo Fisher Scientific, Rockford, Illinois, USA) was performed. Finally, the slides were prepared with mounting media Gel Mount (Sigma–Aldrich, Missouri, USA) and coverslips. The fluorescence intensity was quantified using the software NIS-Elements and Nikon. The autofluorescence rate of each sample was subtracted from the DAF-2 DA and the resulting values were used to evaluate the amount of nitric oxide produced in the tissue.

2.14. Measurement of systemic nitric oxide levels

Plasma levels of NO were estimated from nitrate and nitrite (NOx) quantification as previously described [24]. Briefly, samples were deproteinised by adding zinc sulfate (20 %) in a 1:1 ratio. Then, the

samples were centrifuged (7300 *g* at 4 °C for 15 minutes). The supernatant obtained was incubated with *Escherichia coli* in a 96-well plate at 37 °C per 3 hours to promote the conversion of nitrate into nitrite. Then, samples were centrifuged (2250 *g* for 15 minutes) to remove *bacteria* and the supernatant was mixed with Griess reagent (sulfanilamide 1 %, phosphoric acid 10 %/alpha-naphthyl-ethylenediamine 0.1 % in Milli-Q water) in a 1:1 ratio. The absorbance was read at 540 nm in a 96-well microplate reader (SpectraMax Paradigm, Molecular Devices, CA, USA). Standard curves for nitrate and nitrite (0–150 μM) were included into the plate. Finally, the values were interpolated and expressed as μM of NOx through a linear regression.

2.15. Ex vivo assessment of vascular reactivity

The thoracic aortas obtained from mice at 24 h after CLP or sham surgery were placed in a Petri dish containing ice-cold Krebs solution (concentrations, in mM: NaCl 130.0, KCl 4.7, KH_2PO_4 1.18, $MgSO_4.7\ H_2O$ 1.17, $NaHCO_3$ 14.9, D-glucose 5.5, $CaCl_2.2\ H_2O$ 1.6). Under a stereo microscope, the arteries were carefully cleaned from all connective tissues, and were sectioned into 2–3 mm rings. The aortic rings were mounted in an organ bath system (model 620 M; Danish Myo Technology, Hinnerup, Denmark), allowing the detection of vascular tone, which was recorded using the software LabChart (version 8; ADInstruments, Bella Vista, Australia).

The preparations were subjected to an isometric tension of 0.5 mN, which were maintained throughout the experiment. The arteries were bathed with a warmed (37 ºC) Krebs nutritive solution, continuously bubbled with a carbogenic mixture (95 % O_2/5 % CO_2). After a stabilisation period of 45 min, the vessels were subjected to 1 μM phenylephrine followed by 1 μM acetylcholine to assess the endothelia function. Only arteries showing functional endothelium, characterised by the ability of acetylcholine to induce at least 80 % relaxation in phenylephrine-precontracted rings, were included in our experiments. Baths were then washed, allowed to rest again for 45 min, and concentration-response curves were constructed to evaluate vascular responsiveness to vasoconstrictor and vasodilator agents, including phenylephrine, norepinephrine, acetylcholine, and sodium nitroprusside. The cumulative concentrations used in our study ranged from 1 nM to 30 μM) for all four drugs. Relaxation responsivities were evaluated in vessels pre-contracted with 1 μM phenylephrine. The maximum effect achieved (E_{max}), the half maximum effective concentration (EC_{50}, represented as p EC_{50}) and the area under the curve (AUC) of the vasoactive agents were calculated.

2.16. Statistical analysis

The results are presented as the mean ± standard deviation (S.D.) for the number of animals used in each experimental group. Prior to analysis, data distribution was assessed through the Shapiro-Wilk test, and homogeneity of variances was evaluated using the Bartlett test. Data underwent a logarithmic transformation whenever needed to achieve normality and homogeneity of variance. After confirming these conditions, statistical analysis was conducted employing one-way analysis of variance (ANOVA), followed by the Bonferroni *post-hoc* test. For data sets that remained non-normally distributed or heterogeneous in variance despite the logarithmic transformation, non-parametric statistical methods were employed, specifically the Kruskal-Wallis test followed by Dunn's *post-hoc* test. Concentration-response curves in functional experiments were fitted using nonlinear regression. Agonist potencies and efficacy were expressed as the negative logarithm of the molar concentration of agonist inducing 50 % of the maximum response (pEC50) and the maximum effect elicited by the agonist (E_{max}), respectively. Survival analysis was conducted using the log-rank (Mantel-Cox) test. A significance threshold of $p < 0.05$ was applied. All analyses were executed utilising GraphPad Prism 8.00 software (GraphPad Software, San Diego, CA, USA).

3. Results

3.1. Silmitasertib counteracts sepsis-induced multiorgan failure

Septic mice developed multiorgan failure when compared to Sham-operated mice, as shown by a robust increase in the plasma levels of creatinine and urea, the transaminases AST and ALT, amylase and LDH, suggestive of renal dysfunction, liver and pancreatic injury, respectively. Intriguingly, CLP mice treated with silmitasertib showed a significant reduction in all aforementioned biochemical markers of organ dysfunction, when compared to CLP-mice treated with vehicle (Table 1). Renal dysfunction was further confirmed by evaluating the local expression of KIM-1, a type I transmembrane glycoprotein associated with proximal renal tubular injury, which has been demonstrated to be upregulated following kidney injury [25]. Consistently, as shown in Fig. 1, silmitasertib administration to septic mice reduced the KIM-1 immunopositivity.

3.2. Silmitasertib ameliorates renal perfusion reducing local and systemic nitric oxide production during experimental sepsis

In addition to acute kidney dysfunction, *in vivo* analysis revealed a significant reduction in renal blood flow, with a striking drop in more than 250 PU in septic mice when compared to sham-operated mice (Fig. 2, panel A). Remarkably, the treatment with silmitasertib evoked a 50 % increase in the blood perfusion parameter when compared to CLP untreated mice (Fig. 2A). Simultaneously, vehicle-treated septic mice exhibited a significant increase in DAF-2 fluorescence intensity in the renal tissue when compared to sham-operated mice (Fig. 2B), indicating excessive local NO production, as illustrated by the semi-quantification of relative fluorescence intensity (Fig. 2C). The acute administration of the CK2 inhibitor silmitasertib in septic mice significantly blunted this increase, resulting in fluorescence levels not different from those observed in sham-operated mice. Interestingly, the increase in the local NO levels in kidneys was paralleled by a robust rise in plasma NOx levels, which was also significantly mitigated by silmitasertib administration (Fig. 2D).

3.3. Silmitasertib mitigates the overactivation of the CK2/NF-κB/iNOS pathway in the kidney of septic mice

In order to deepen the molecular mechanism(s) underlying the renoprotective effects of silmitasertib during sepsis, we performed qRT-PCR and western blot analysis in kidney tissue samples. The qRT-PCR analysis demonstrated that neither sepsis nor silmitasertib treatment interfered with the expression of the CSNK2α1 gene, when compared to

Table 1
Effects of silmitasertib on plasma biomarkers of sepsis-induced multiorgan dysfunction.

Biomarkers	Sham	CLP	CLP + Silm
Creatinine (mg/dL)	0.38 ± 0.09	0.64 ± 0.18*	0.42 ± 0.10$^{\#}$
Urea (mg/dL)	30.37 ± 12.86	133.4 ± 112.5*	29.27 ± 20.48$^{\#}$
AST (U/L)	9.17 ± 0.92	49.23 ± 26.09*	28.55 ± 10.45$^{*\#}$
ALT (U/L)	5.84 ± 1.64	25.61 ± 19.85*	12.02 ± 5.56$^{*\#}$
Amylase (U/L)	360.6 ± 95.99	541.9 ± 121.8*	374.5 ± 120.1$^{\#}$
LDH (U/L)	30.03 ± 4.18	162.8 ± 82.71*	77.34 ± 45.77$^{*\#}$

Mice were randomly assigned to undergo Sham or CLP surgery. One-hour post-surgery, CLP mice received once either vehicle (PBS) or Silm (50 mg/kg i.v.). Twenty-four hours after the sham or CLP procedure, plasma concentrations of creatinine, urea, aspartate aminotransferase (AST), alanine aminotransferase (ALT), amylase and lactate dehydrogenase (LDH) were quantified. Data are shown as mean ± S.D. for groups of 8–10 mice. Statistical analysis was conducted utilising one-way ANOVA followed by Bonferroni's post-test. Significance levels ($p < 0.05$) were denoted as * for CLP and CLP+Silm *vs* Sham, and $^{\#}$ for CLP+Silm *vs* CLP.

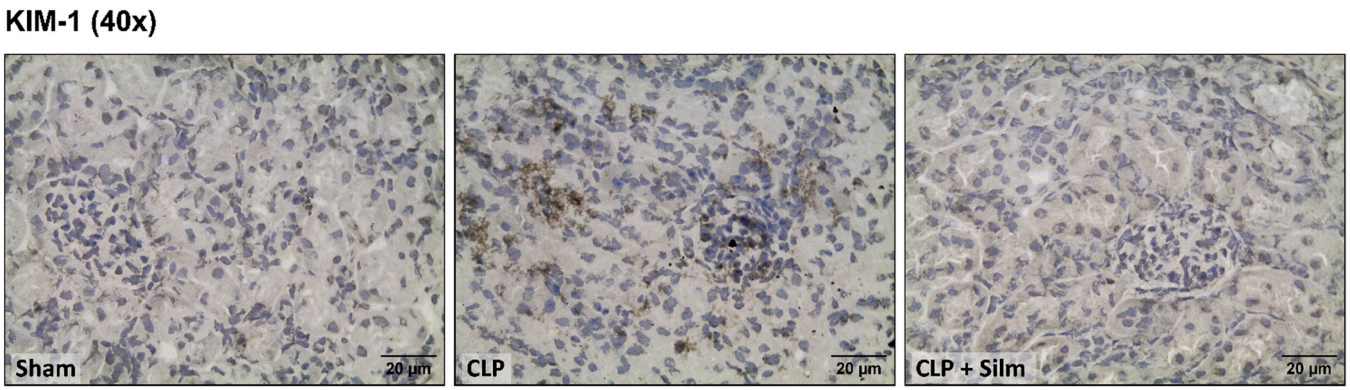

Fig. 1. Assessment of KIM-1 expression in renal sections of septic mice. Mice were randomly assigned to undergo Sham or CLP surgery. One-hour post-surgery, CLP mice received once either vehicle (PBS) or Silm (50 mg/kg i.v.). Twenty-four hours after Sham or CLP procedure, kidney samples were harvested. Renal tissue sections were prepared to identify kidney injury molecule-1 (KIM-1) through immunohistochemistry assay. Representative photomicrographs at 40x magnification were determining using 5 animals per group.

Sham-operated mice (Fig. 3A), which was confirmed by the lack of modulation in the protein expression of total CK2α (Fig. 3B). However, compared to Sham-operated mice, vehicle-treated CLP-mice displayed substantial increment in renal CK2α phosphorylation at Tyr^{255}, a finding suggestive of enzyme activation. Most notably, treatment of CLP-mice with silmitasertib significantly attenuated the abnormal activation of CK2 during sepsis (Fig. 3B). Sepsis-induced CK2 overactivation was associated with the activation of the NF-κB pathway, as documented by increased phosphorylation of IKKα/β at $Ser^{176/180}$ (Fig. 3C), enhanced phosphorylation of IκBα at $Ser^{32/36}$ (Fig. 3D), culminating in augmented nuclear translocation of the p50 NF-κB subunit (Fig. 3E). The activation of this transcription factor resulted in the overexpression of the NF-κB-dependent enzyme iNOS (Fig. 3F). Most notably, attenuated CK2 activation following silmitasertib administration blunted both expression and activation of markers of the NF-κB/iNOS axis, thus explaining, at least in part, its beneficial role in interfering with sepsis-related excessive NO production. We also extended our investigation to another inflammatory pathway involved in sepsis, whose expression is affected by NF-κB activation, namely the NLRP3 inflammasome complex. As shown in the Suppl. Fig.1, vehicle-treated CLP-mice exhibited significantly increased renal expression of NLRP3 inflammasome, cleaved caspase-1 and IL-1β, which were significantly attenuated in septic mice treated with silmitasertib.

3.4. Silmitasertib reduces sepsis-induced arterial NO release thus improving vascular impairment in response to vasoactive drugs

To further extend our investigation on the potential vasoactive properties of silmitasertib, we performed analysis on aorta sections, showing silmitasertib ability to interfere with arterial NO release evoked by sepsis (Fig. 4A-B). Sequentially, conductance arteries were isolated to assess vascular responsiveness in experimental sepsis. Aortic rings from mice subjected to CLP showed a significant reduction in phenylephrine-induced contractility when compared to aortas from sham-operated mice (Fig. 5A). As shown in Table 2, the septic insult reduced the potency (pEC50), the efficacy (E_{max}) and the corresponding AUC for the response to phenylephrine. Interestingly, treatment with silmitasertib massively counteracted the sepsis-induced vascular hyporesponsiveness to phenylephrine. Similar results were obtained when the aortic rings were challenged with norepinephrine (Fig. 5B) despite the lack of statistical significance on the pEC50 ($p = 0.08$, CLP *vs* CLP + Silm) (Table 2). As shown in the Suppl. Fig. 2 and Suppl. Table 1, silmitasertib administration to septic mice also alleviated vascular impairments due to exposure to vasodilators (acetylcholine and sodium nitroprusside).

3.5. Silmitasertib improves short-term clinical outcomes, thereby prolonging the survival of septic mice

As shown in Fig. 6, at 24 h follow-up evaluation, septic mice showed a massive increase in the systemic levels of several cytokines, including IL-1β, IL-6, TNF-α, IL-17, IFN-γ and IL-10. The cytokine storm was significantly counteracted by silmitasertib administration. This beneficial effect was paralleled by a significant improvement of the markers of severity scores and body temperature, indicating a rapid improvement in the health status of septic mice treated with silmitasertib (Figs. 7A and 7B). Survival analysis demonstrated that the beneficial effects of the acute administration of silmitasertib were maintained over time. In fact, while septic mice showed a high mortality rate throughout the study, with almost 90 % mortality at 120 hours post-surgery, silmitasertib-treated CLP-mice showed impressively prolonged survival, accounting for only 30 % of mortality at the time-point 120 hours (Fig. 7C).

4. Discussion

The quest for novel selective pharmacological approaches in sepsis is an imperative undertaking, yet it poses considerable challenges, particularly concerning the failure of translational research [26]. We hypothesise that proposing selective drugs interfering with mechanisms arising during both sepsis and septic shock (circulatory collapse) stages would be able to potentially ameliorate septic outcomes, thereby, representing a robust approach to ensuring success in translational research. Here, we investigated the beneficial effects of silmitasertib, a highly selective and potent CK2α inhibitor, to counteract acute hyperinflammation and circulatory collapse in an experimental model of sepsis induced by CLP. In the present trial, we reported, for the first time, that CK2 is overactivated during sepsis, thus contributing, at least partially, to systemic hyperinflammation, which culminates with circulatory collapse (manifested by tissue hypoperfusion and arterial hyporesponsiveness to vasoconstrictors), ultimately resulting in multiorgan failure and death. Conversely, pharmacological inhibition with silmitasertib mitigated sepsis-induced acute hyperinflammation and septic shock features, including improved tissue perfusion and vascular reactivity to vasoconstrictors, thereby reducing multiorgan dysfunction and enhancing short-term outcomes. Most notably, the short-term outcomes were importantly translated to long-term protective effects, as evidenced by the prolonged survival of septic mice.

Even though several studies have recently documented increased expression and activity of CK2 in inflammatory and hypoxic conditions, including psoriasis [27], rheumatoid arthritis [16], glomerulonephritis [28] and renal ischemia/reperfusion injury [17], this is the first *in vivo* study investigating the role of CK2 in sepsis, focusing on the effects of its

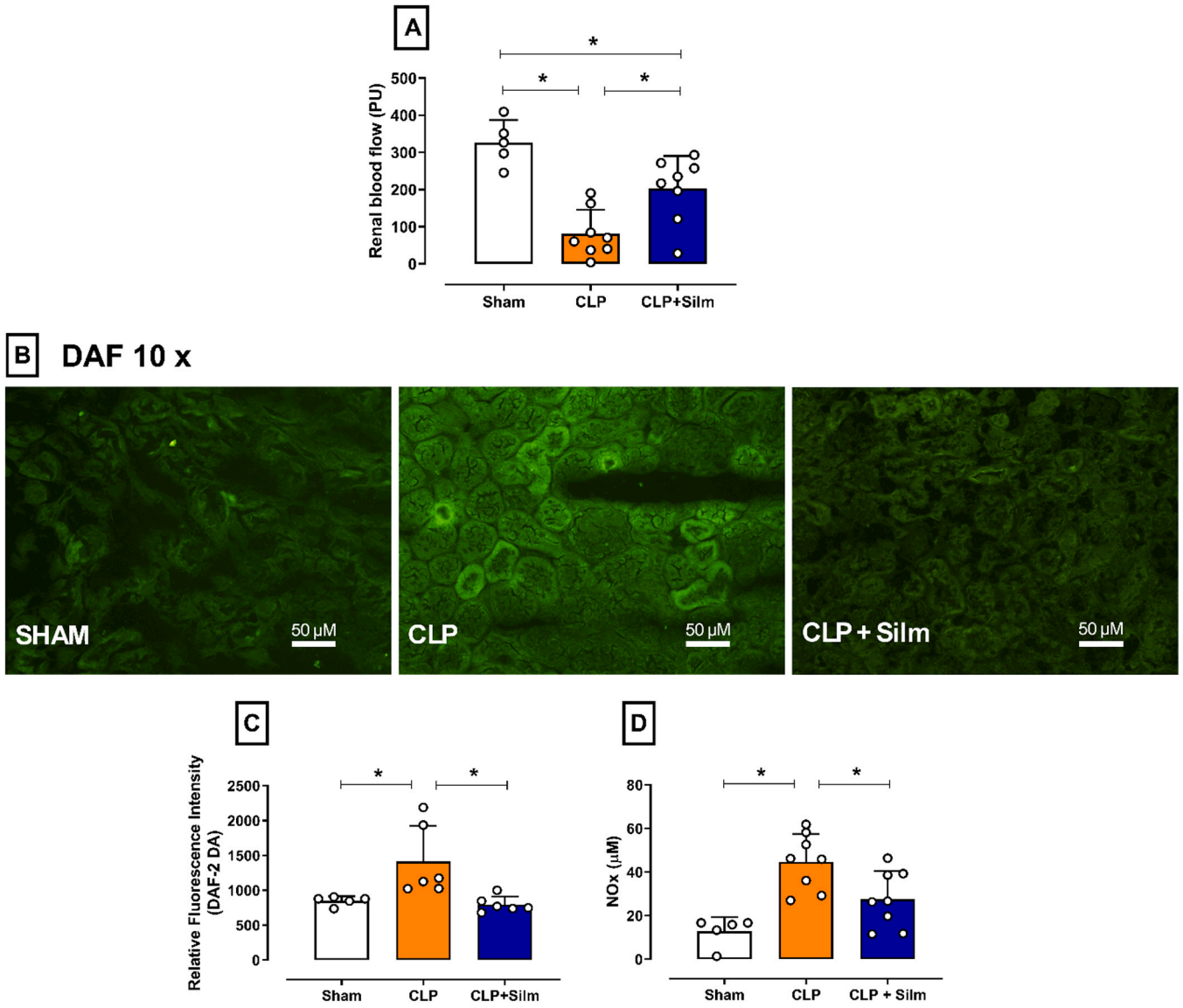

Fig. 2. Renal blood flow analysis and renal and systemic NO release assessment during experimental sepsis. Mice were randomly assigned to undergo sham or CLP surgery. One-hour post-surgery, CLP mice received a single administration of either vehicle (PBS) or Silm (50 mg/kg i.v.). Twenty-four hours after sham or CLP procedure, (A) renal blood flow (RBF) was recorded *in vivo*, then plasma and kidneys were harvested for analysis. Renal tissue sections were prepared to identify NO using DAF-2 DA probe. (B) Representative photomicrographs at 10x magnification were obtained from 5 to 6 animals per group. (C) Semi-quantitative analysis of the relative fluorescence intensity of DAF-2 DA (AU) in renal tissue sections and (D) systemic levels of nitrate + nitrite (NOx), as measured in plasma samples. Data are expressed as dot plots for each animal and as mean ± S.D. of 5–8 mice per group. Statistical analysis was conducted utilising one-way ANOVA followed by Bonferroni's post-test. Significance levels were denoted as *$p < 0.05$.

pharmacological inhibition by silmitasertib, a potent, selective, and ATP-competitive inhibitor of CK2α. Despite the lack of histopathological analysis in different organs, the significant changes in the concentration levels of selective markers of organ injury detected following silmitasertib administration are suggestive of drug protective effects against multiorgan failure. Most notably, we observed a significant drug-induced improvement in biomarkers of renal dysfunction (creatinine and urea) and hypoperfusion, which was further confirmed by the reduced expression of KIM-1, a type I transmembrane glycoprotein linked to damage in the proximal renal tubules, whose levels directly correlate with sepsis-associated kidney dysfunction [29]. These findings are particularly noteworthy given the pivotal role of the renal system in the pathophysiology of sepsis [30]. In the kidneys of septic mice, we also documented an overactivation of CK2 following the septic insult, which was drastically inhibited by silmitasertib. Overall, these findings highlight the relevance of the kidney as one of the main targets of the proposed pharmacological approach and suggest a role for CK2 in the sepsis pathogenesis.

As previously documented [31,32], lipopolysaccharide (LPS) and pro-inflammatory cytokines, including IL-1β and IL-6, can evoke CK2 overactivation. In turn, CK2 can activate the pro-inflammatory NF-κB pathway [33], whose detrimental role in the disease progression has been widely documented [34]. Here we confirmed the crosstalk linking CK2 activation to NF-κB nuclear translocation, and we demonstrated that CK2 inhibition was paralleled by reduced activation of markers of the NF-κB cascade, strengthening the hypothesis that CK2 contributes to septic inflammation in an NF-κB-dependent manner. Our findings are in keeping with previous studies showing that CK2 directly phosphorylates the IKK, IκBα and p65 subunits of the NF-κB complex, thereby enabling the initiation of the inflammatory cascade [15,35,36]. Besides, CK2 can foster inflammation by inhibiting the activity of repressor proteins, such as the phosphorylating somatic nuclear autoantigenic sperm protein

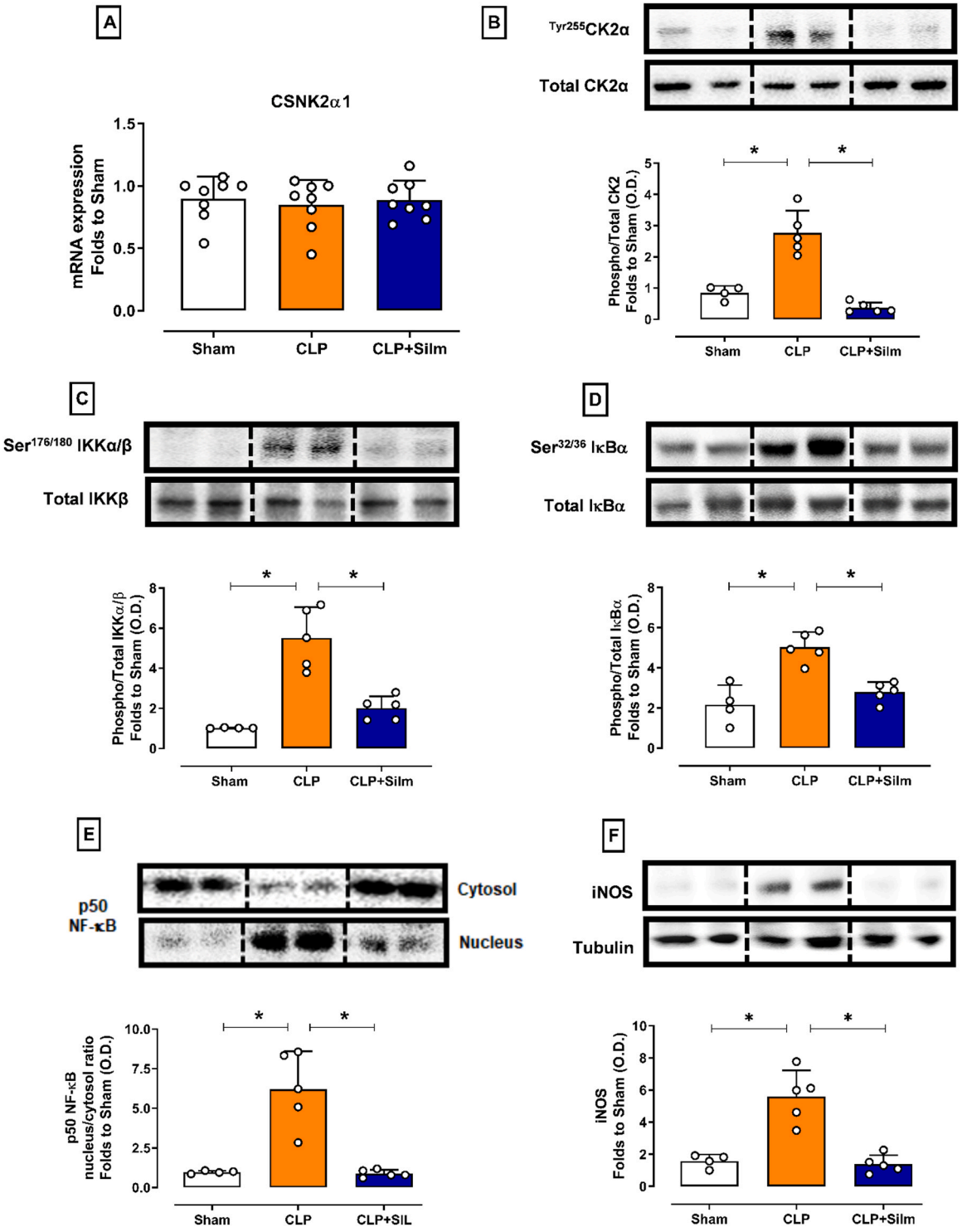

Fig. 3. Biomolecular analysis of CK2/NF-κB/iNOS axis during experimental sepsis. Mice were randomly assigned to undergo Sham or CLP surgery. One hour post-surgery, CLP mice received once either vehicle (PBS) or Silm (50 mg/kg i.v.). Twenty-four hours after sham or CLP procedure, kidneys were harvested for molecular analysis. (A) CSNK2α1 gene expression was quantified by real-time PCR following the extraction of total mRNA from kidney samples. Relative gene expression was determined through normalisation with housekeeping genes (18 S and GAPDH). The formula $2^{-\Delta\Delta CT}$ was employed to determine the fold change compared to the sham group. (B) The phosphorylation of CK2α at Tyr^{255}; (C) the phosphorylation of IKKα/β at $Ser^{176/180}$; (D) the phosphorylation of IκBα at $Ser^{32/36}$; (E) the nuclear translocation of p50 and (F) the expression of iNOS were determined by western blotting. Densitometric analysis of the bands are expressed as relative optical density (O.D.) and normalised to the sham band. Data are expressed as dot plots for each animal and as mean ± S.D. of 4–8 mice per group. Statistical analysis was conducted utilising one-way ANOVA followed by Bonferroni's post-test. Significance levels were denoted as *$p < 0.05$.

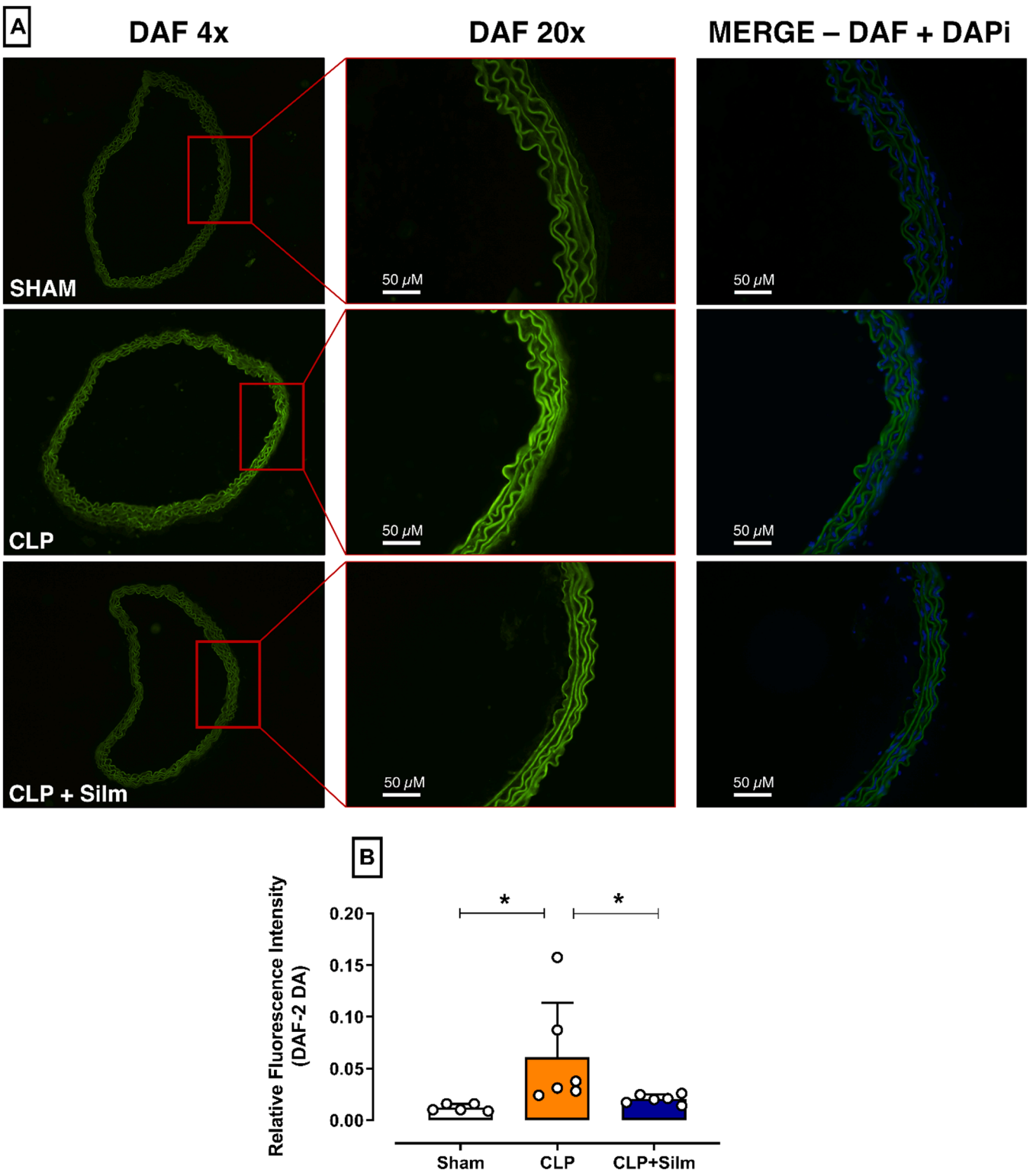

Fig. 4. Assessment of arterial NO production in septic mice. Mice were randomly assigned to undergo Sham or CLP surgery. One hour post-surgery, CLP mice received once either vehicle (PBS) or Silm (50 mg/kg i.v.). Twenty-four hours after sham or CLP procedure, thoracic aorta samples were analysed. Tissue sections were prepared to identify NO release in the aortas using a DAF-2 DA probe. (A) Representative photomicrographs at 4x and 10x magnification were recorded. (B) Semi-quantitative analysis of the relative fluorescence intensity of DAF-2 DA (AU) is expressed as dot plots for each animal and as mean ± S.D. of 5–6 mice per group. Statistical analysis was conducted utilising one-way ANOVA followed by Bonferroni's post-test. Significance levels were denoted as *$p < 0.05$.

(sNASP) [37] and the transcription factor activating transcription factor 3 (ATF3) [38], thus resulting in an increased transcriptional activity of inflammatory genes.

The NLRP3 inflammasome is one of the main inflammatory proteins, whose gene expression relies on NF-κB transcriptional activity and that exerts a pivotal role in the context of sepsis-induced multiorgan failure [39,40]. Here we demonstrated that the inhibition of CK2-NFkB pathway by silmitasertib resulted in a reduced expression of NLRP3 as

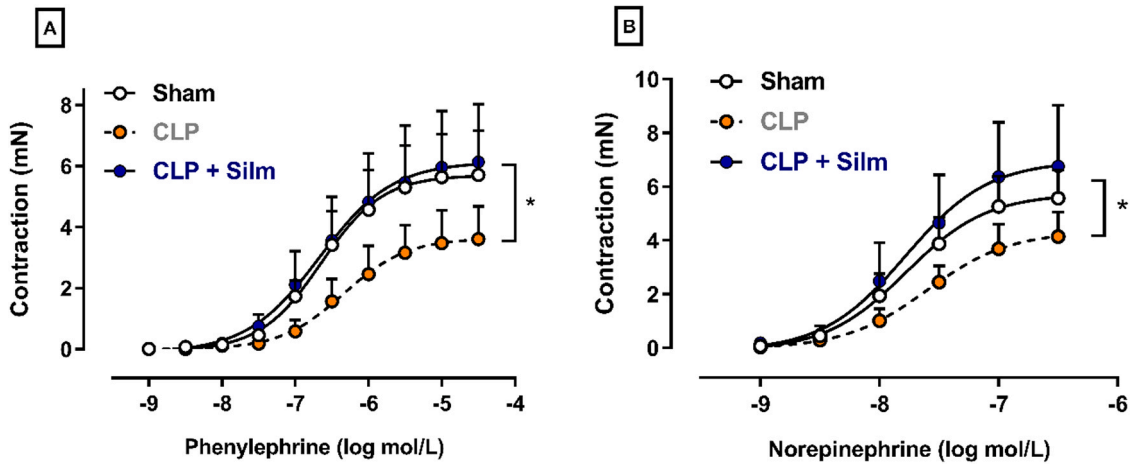

Fig. 5. ***Ex vivo*** **analysis of vascular response to vasoconstrictors in septic mice.** Mice were randomly assigned to undergo sham or CLP surgery. One hour post-surgery, CLP mice received once either vehicle (PBS) or Silm (50 mg/kg i.v.). Twenty-four hours after sham or CLP procedure, the thoracic aorta was collected and mounted in an organ bath system. Cumulative concentration-response curves were determined for (A) phenylephrine and (B) norepinephrine. Data are expressed as mean ± S.D. of 5–8 mice per group. Statistical analysis was conducted utilising one-way ANOVA followed by Bonferroni's post-test. Significance levels were denoted as *p < 0.05 CLP and CLP+Silm *vs* Sham. #p < 0.05 CLP+Silm *vs* CLP.

Table 2
Effects of silmitasertib on *ex vivo* potency and efficacy of vasoconstrictors during experimental sepsis.

		Sham	CLP	CLP + Silm
Phenylephrine	pEC_{50}	6.63 ± 0.13	6.34 ± 0.23*	6.65 ± 0.22#
	E_{max} (g)	5.72 ± 1.36	3.72 ± 1.15*	6.12 ± 1.83#
	AUC (AU)	12.1 ± 3.22	6.94 ± 2.42*	13.03 ± 4.38#
Norepinephrine	pEC_{50}	7.77 ± 0.09	7.59 ± 0.12	7.76 ± 0.16
	E_{max} (g)	5.72 ± 1.07	4.37 ± 1.03	6.93 ± 2.36#
	AUC (AU)	7.17 ± 1.76	4.77 ± 1.21	8.78 ± 3.32#

Mice were randomly assigned to undergo sham or CLP surgery. One-hour post-surgery, CLP mice received once either vehicle (PBS) or Silm (50 mg/kg i.v.). Twenty-four hours after Sham or CLP procedure, the thoracic aorta was collected and mounted in an organ bath system. Cumulative concentration-response curves were determined for phenylephrine and norepinephrine. The pEC50 represents the negative logarithm of the drug concentration that gives the half-maximal effective concentration (EC50). E_{max} refers to the maximum effect achieved. AUC refers to the area under the curve. Data are expressed as mean ± S.D. of 5–8 animals per group. Statistical analysis was conducted utilising one-way ANOVA followed by Bonferroni's post-test. Significance levels were denoted as *p < 0.05 CLP *vs* Sham; #p < 0.05 CLP+Silm *vs* CLP.

well as reduced activation of the NLRP3 inflammasome complex, as suggested by reduction in cleaved caspase-1 and IL-1β release. Altogether, this dataset is consistent with the reduced systemic inflammatory scenario orchestrated by the sepsis-induced cytokine storm, which we detected following silmitasertib administration. This broad anti-inflammatory impact of CK2 inhibition is unlikely to be limited solely to the NF-κB and NLRP3 pathways. As previously documented [41], alternative pathways may contribute to the molecular pathophysiology of sepsis. Along with NF-κB, other transcription factor activators, such as the activator protein-1 (AP-1), are involved in the development of immune and inflammatory responses associated with sepsis [42]. Similarly, the pathogenetic role of the JAK-STAT cascade, which acts as a downstream effector of cytokine receptors, in the development of key organ dysfunction in sepsis has already been documented [13,14]. Moreover, the selective inhibition of STAT3 transcriptional activity has shown significant protective effects in mice with CLP-induced sepsis [43]. Thus, we must acknowledge that additional mechanisms may contribute to the amelioration of organ perfusion induced by CK2 inhibition and further investigations are needed to better elucidate the cross-talk mechanism(s), if any, linking CK2 activity to the modulation of the above-mentioned signalling pathways within the complex and multifaceted pathogenesis of sepsis.

To investigate the potential direct impact of drug treatment on local and systemic haemodynamic properties, we measured changes in the NO levels in both kidney and thoracic aorta samples. NO exerts a well-established pathological role in hemodynamic imbalance during sepsis [44,45]. As we documented, NO levels were drastically increased in septic mice, and this increase was due, at least in part, to an over-expression of the NF-κB-dependent protein iNOS. Most notably, we demonstrated that silmitasertib effectively attenuated the iNOS-NO axis, thus facilitating enhancements in organ perfusion. Beyond its well-known vasorelaxant properties, NO also exerts substantial impact on the desensitisation of the adrenergic receptors, and this phenomenon massively contributes to the hyporesponsiveness to vasopressor therapy often detected in the clinical settings of sepsis [46,47]. In addition to the beneficial effects of reducing renal and systemic NO release, silmitasertib evoked a massive decrease in NO levels in the arteries. This finding suggests a potential positive influence on adrenergic response to vasoactive drugs. Indeed, when we evaluated the vascular reactivity to vasoconstrictors (phenylephrine and norepinephrine), we observed that the silmitasertib treatment importantly restored the vasoreactivity response to vasoconstrictors impaired by sepsis. These findings further strengthen the potential clinical relevance of silmitasertib in the context of septic shock, as the goal of reaching and maintaining mean arterial pressure above 65 mmHg in clinical settings remains challenging, largely due to the ineffectiveness of vasopressor therapy [5,48]. Furthermore, our results suggest that the vascular beneficial effects of silmitasertib are exerted mainly on the endothelium, as evidenced by the responses detected in arterial segments exposed to acetylcholine and sodium nitroprusside challenges.

5. Conclusions

Our results suggest, for the first time, a pivotal role of CK2 in sepsis pathogenesis and, most notably, demonstrate the beneficial effects of its pharmacological targeting in septic mice. Specifically, we showed that the acute administration of the selective CK2 inhibitor silmitasertib exerts protection against the hyperinflammatory storm and vascular activity, leading to clinically relevant haemodynamic changes. Overall, these effects significantly contribute to evoking a robust reduction in sepsis mortality, thus indicating silmitasertib as a powerful original pharmacological approach to be considered for drug repurposing in sepsis.

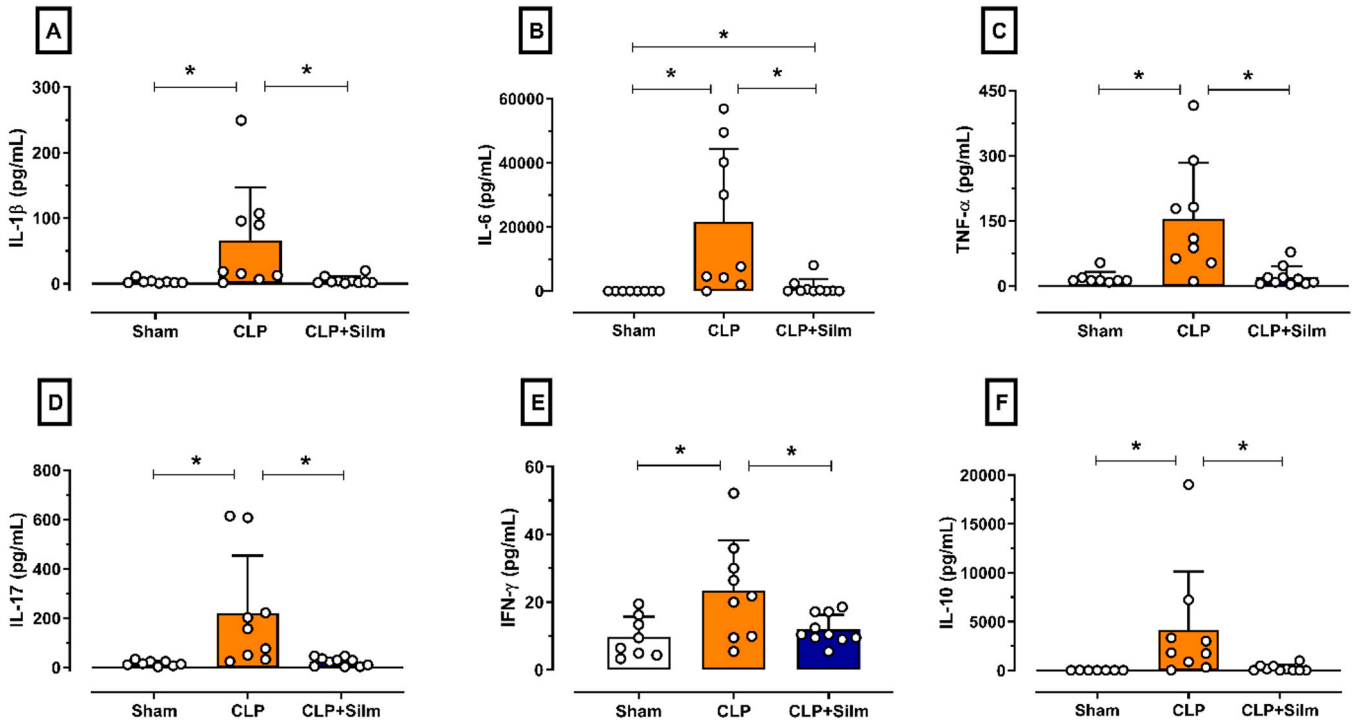

Fig. 6. Effects of silmitasertib on systemic cytokine storm evoked by experimental sepsis. Mice were randomly assigned to undergo sham or CLP surgery. One hour post-surgery, CLP mice received once either vehicle (PBS) or Silm (50 mg/kg i.v.). Twenty-four hours after sham or CLP procedure, plasma levels of (A) IL-1β, (B) IL-6, (C) TNF-α, (D) IL-17, (E) IFN-γ and (F) IL-10 were determined. Data are expressed as dot plots for each animal and as mean ± S.D. of 8–10 mice per group. IL-1β, IL-6, TNF-α, IL-17 and IFN-γ and were analysed by one-way ANOVA followed by Bonferroni's post-test, while IL-10 was analysed by Kruskal-Wallis followed by Dunn's post-test. Significance levels were denoted as *p < 0.05.

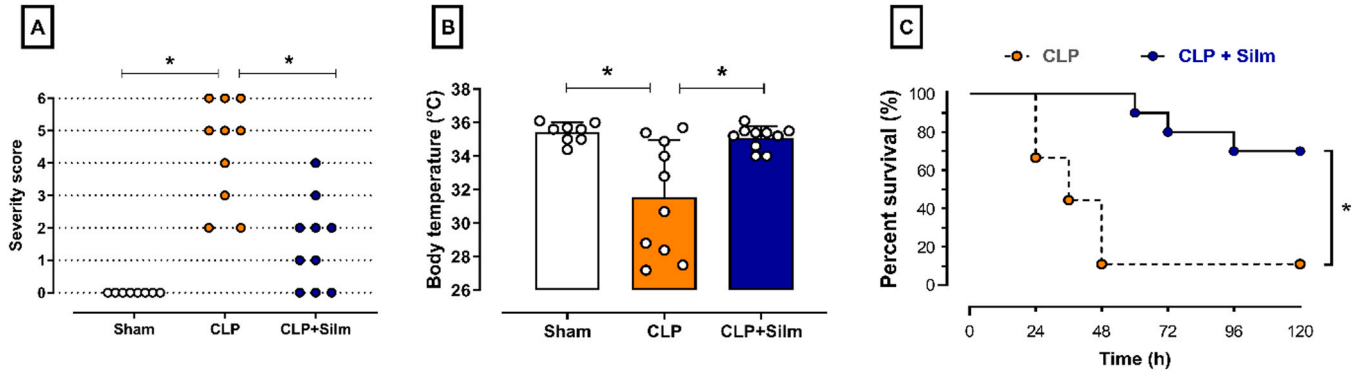

Fig. 7. Effects of silmitasertib on clinical score, body temperature and survival in septic mice. Mice were randomly assigned to undergo sham or CLP surgery. One-hour post-surgery, CLP mice received once either vehicle (PBS) or Silm (50 mg/kg i.v.). Twenty-four hours after sham or CLP procedure, (A) severity score and (B) body temperature were recorded. Data are expressed as dot plots for each animal and as mean ± S.D. of 8–10 mice per group. The Kruskal-Wallis followed by Dunn's post-test was applied to assess the severity score, whereas for body temperature, one-way ANOVA followed by Bonferroni's post-test was used. Significance levels were denoted as *p < 0.05. (C) The survival study was carried out for 120 hours. A log-rank test was used to compare the survival curves (n = 14 mice per group). *p < 0.05 CLP vs CLP+Silm.

Ethical Statement

All *in vivo* experiments conducted in this study adhered to the guidelines set forth by the local Animal Use and Care Committees, as well as the National Authorities (Ethical license numbers: 855/2021-PR, Italy and 7982210222-UFSC, Brazil). The protocols employed are in strict accordance with the ARRIVE guidelines [19] and the MQTiPSS recommendations for preclinical sepsis studies [20].

CRediT authorship contribution statement

Massimo Collino: Writing – review & editing, Supervision, Funding acquisition, Conceptualization. **Eleonora Aimaretti:** Visualization, Validation, Investigation. **Maria Luísa da Silveira Hahmeyer:** Validation, Methodology, Investigation. **Giacomo Einaudi:** Validation, Investigation. **Elisa Porchietto:** Validation, Investigation. **Chiara Rubeo:** Validation, Investigation. **Enrica Marzani:** Validation, Investigation. **Manuela Aragno:** Writing – review & editing, Resources. **José Eduardo da Silva-Santos:** Writing – review & editing, Validation. **Carlo Cifani:** Writing – review & editing, Resources, Funding acquisition. **Daniel Fernandes:** Writing – review & editing, Validation, Supervision, Resources, Funding acquisition. **Gustavo Ferreira Alves:** Writing – original draft, Visualization, Validation, Investigation, Formal analysis, Data curation, Conceptualization.

Declaration of Competing Interest

The authors have declared no conflict of interest.

Data availability

Data will be made available on request.

Acknowledgment(s)

This work has received funding from the Italian Ministry for University and Research in the framework of the 2022 Program for Research Projects of National Interest (PRIN) under Grant 20224PR8HE and Conselho Nacional de Desenvolvimento Científico e Tecnológico (CNPq, Brazil) under Grant 403.615/2023–2. We would like to thank Prof. Geisson Marcos Nardi for his expertise and assistance in performing the immunohistochemistry assays.

Appendix A. Supporting information

Supplementary data associated with this article can be found in the online version at doi:10.1016/j.biopha.2024.117191.

References

[1] K.E. Rudd, S.C. Johnson, K.M. Agesa, et al., Global, regional, and national sepsis incidence and mortality, 1990–2017: analysis for the Global Burden of Disease Study, Lancet 395 (2020) 200–211.
[2] J. Cavaillon, M. Singer, T. Skirecki, Sepsis therapies: learning from 30 years of failure of translational research to propose new leads, Epub ahead of print 7, EMBO Mol. Med. 12 (April 2020), https://doi.org/10.15252/emmm.201810128. Epub ahead of print 7.
[3] L. Evans, A. Rhodes, W. Alhazzani, et al., Surviving Sepsis Campaign: International Guidelines for Management of Sepsis and Septic Shock 2021, Crit. Care Med. 49 (2021) e1063–e1143.
[4] S. Lambden, B.C. Creagh-Brown, J. Hunt, et al., Definitions and pathophysiology of vasoplegic shock, Crit. Care 22 (2018) 174.
[5] M. Singer, C.S. Deutschman, C.W. Seymour, et al., The Third International Consensus Definitions for Sepsis and Septic Shock (Sepsis-3), JAMA 315 (2016) 801.
[6] G.F. Alves, E. Aimaretti, G. Einaudi, et al., Pharmacological Inhibition of FAK-Pyk2 Pathway Protects Against Organ Damage and Prolongs the Survival of Septic Mice, Epub ahead of print 1, Front. Immunol. 13 (February 2022), https://doi.org/10.3389/fimmu.2022.837180. Epub ahead of print 1.
[7] C.E. O'Riordan, G.S.D. Purvis, D. Collotta, et al., X-Linked Immunodeficient Mice With No Functional Bruton's Tyrosine Kinase Are Protected From Sepsis-Induced Multiple Organ Failure, Epub ahead of print 7, Front. Immunol. 11 (October 2020), https://doi.org/10.3389/fimmu.2020.581758. Epub ahead of print 7.
[8] C. Verra, S. Mohammad, G.F. Alves, et al., Baricitinib protects mice from sepsis-induced cardiac dysfunction and multiple-organ failure, Epub ahead of print 12, Front. Immunol. 14 (September 2023), https://doi.org/10.3389/fimmu.2023.1223014. Epub ahead of print 12.
[9] H.J. Chon, K.J. Bae, Y. Lee, et al., The casein kinase 2 inhibitor, CX-4945, as an anti-cancer drug in treatment of human hematological malignancies, Epub ahead of print 31, Front. Pharmacol. 6 (March 2015), https://doi.org/10.3389/fphar.2015.00070. Epub ahead of print 31.
[10] C. Borgo, C. D'Amore, S. Sarno, et al., Protein kinase CK2: a potential therapeutic target for diverse human diseases, Signal Transduct. Target Ther. 6 (2021) 183.
[11] Y. Zheng, B.C. McFarland, D. Drygin, et al., Targeting Protein Kinase CK2 Suppresses Prosurvival Signaling Pathways and Growth of Glioblastoma, Clin. Cancer Res. 19 (2013) 6484–6494.
[12] J.S. Bae, S. Park, K.M. Kim, et al., CK2α phosphorylates DBC1 and is involved in the progression of gastric carcinoma and predicts poor survival of gastric carcinoma patients, Int. J. Cancer 136 (2015) 797–809.
[13] Y. Zheng, H. Qin, S.J. Frank, et al., A CK2-dependent mechanism for activation of the JAK-STAT signaling pathway, Blood 118 (2011) 156–166.
[14] U. Rozovski, D.M. Harris, P. Li, et al., Constitutive Phosphorylation of STAT3 by the CK2–BLNK–CD5 Complex, Mol. Cancer Res. 15 (2017) 610–618.
[15] C.F. Barroga, J.K. Stevenson, E.M. Schwarz, et al., Constitutive phosphorylation of I kappa B alpha by casein kinase II, Proc. Natl. Acad. Sci. 92 (1995) 7637–7641.
[16] Y. Luo, Y. Lei, X. Guo, et al., CX-4945 inhibits fibroblast-like synoviocytes functions through the CK2-p53 axis to reduce rheumatoid arthritis disease severity, Int. Immunopharmacol. 119 (2023) 110163.
[17] S.-O. Ka, H.P. Hwang, J.-H. Jang, et al., The protein kinase 2 inhibitor tetrabromobenzotriazole protects against renal ischemia reperfusion injury, Sci. Rep. 5 (2015) 14816.
[18] F. Pierre, P.C. Chua, S.E. O'Brien, et al., Pre-clinical characterization of CX-4945, a potent and selective small molecule inhibitor of CK2 for the treatment of cancer, Mol. Cell Biochem. 356 (2011) 37–43.
[19] N. Percie du Sert, V. Hurst, A. Ahluwalia, et al., The ARRIVE guidelines 2.0: Updated guidelines for reporting animal research, PLoS Biol. 18 (2020) e3000410.
[20] M.F. Osuchowski, A. Ayala, S. Bahrami, et al., Minimum Quality Threshold in Pre-Clinical Sepsis Studies (MQTiPSS): An International Expert Consensus Initiative for Improvement of Animal Modeling in Sepsis, Shock 50 (2018) 377–380.
[21] K.A. Wichterman, A.E. Baue, I.H. Chaudry, Sepsis and septic shock—A review of laboratory models and a proposal, J. Surg. Res. 29 (1980) 189–201.
[22] A. Richter, S. Sender, A. Lenz, et al., Influence of Casein kinase II inhibitor CX-4945 on BCL6-mediated apoptotic signaling in B-ALL in vitro and in vivo, BMC Cancer 20 (2020) 184.
[23] K.J. Livak, T.D. Schmittgen, Analysis of Relative Gene Expression Data Using Real-Time Quantitative PCR and the 2−ΔΔCT Method, Methods 25 (2001) 402–408.
[24] D.L. Granger, J.B. Hibbs, J.R. Perfect, et al., Metabolic fate of L-arginine in relation to microbiostatic capability of murine macrophages, J. Clin. Investig. 85 (1990) 264–273.
[25] Y. Xie, P. Huang, J. Zhang, et al., Biomarkers for the diagnosis of sepsis-associated acute kidney injury: systematic review and meta-analysis, Ann. Palliat. Med. 10 (2021) 4159–4173.
[26] J. Cavaillon, M. Singer, T. Skirecki, Sepsis therapies: learning from 30 years of failure of translational research to propose new leads, Epub ahead of print 7, EMBO Mol. Med. 12 (April 2020), https://doi.org/10.15252/emmm.201810128. Epub ahead of print 7.
[27] W. Huang, X. Zheng, Q. Huang, et al., Protein Kinase CK2 Promotes Proliferation, Abnormal Differentiation, and Proinflammatory Cytokine Production of Keratinocytes via Regulation of STAT3 and Akt Pathways in Psoriasis, Am. J. Pathol. 193 (2023) 567–578.
[28] M. Yamada, S. Katsuma, T. Adachi, et al., Inhibition of protein kinase CK2 prevents the progression of glomerulonephritis, Proc. Natl. Acad. Sci. 102 (2005) 7736–7741.
[29] J.F. Brozat, N. Harbalioğlu, P. Hohlstein, et al., Elevated Serum KIM-1 in Sepsis Correlates with Kidney Dysfunction and the Severity of Multi-Organ Critical Illness, Int. J. Mol. Sci. 25 (2024) 5819.
[30] A. Zarbock, M.K. Nadim, P. Pickkers, et al., Sepsis-associated acute kidney injury: consensus report of the 28th Acute Disease Quality Initiative workgroup, Nat. Rev. Nephrol. 19 (2023) 401–417.
[31] T.K. Means, T.A. Lodie, M.J. Fenton, Activation of protein kinase CK2 by LPS is mediated by the MAP kinase pathway, J. Endotoxin Res. 5 (1999) 37–40.
[32] S. Koch, C.T. Capaldo, R.S. Hilgarth, et al., Protein kinase CK2 is a critical regulator of epithelial homeostasis in chronic intestinal inflammation, Mucosal Immunol. 6 (2013) 136–145.
[33] I. Dominguez, G.E. Sonenshein, D.C. Seldin, Protein Kinase CK2 in Health and Disease, Cell. Mol. Life Sci. 66 (2009) 1850–1857.
[34] J. Chen, J.E. Kieswich, F. Chiazza, et al., IκB Kinase Inhibitor Attenuates Sepsis-Induced Cardiac Dysfunction in CKD, J. Am. Soc. Nephrol. 28 (2017) 94–105.
[35] A. Chantôme, A. Pance, N. Gauthier, et al., Casein Kinase II-mediated Phosphorylation of NF-κB p65 Subunit Enhances Inducible Nitric-oxide Synthase Gene Transcription in Vivo, J. Biol. Chem. 279 (2004) 23953–23960.
[36] S.F. Eddy, S. Guo, E.G. Demicco, et al., Inducible IκB Kinase/IκB Kinase ε Expression Is Induced by CK2 and promotes aberrant nuclear factor-κB activation in breast cancer cells, Cancer Res. 65 (2005) 11375–11383.
[37] F.-M. Yang, Y. Zuo, W. Zhou, et al., sNASP inhibits TLR signaling to regulate immune response in sepsis, J. Clin. Investig. 128 (2018) 2459–2472.
[38] D.H. Jung, K.-H. Kim, H.E. Byeon, et al., Involvement of ATF3 in the negative regulation of iNOS expression and NO production in activated macrophages, Immunol. Res. 62 (2015) 35–45.
[39] V. Kumar, Inflammasomes: Pandora's box for sepsis, J. Inflamm. Res. Volume 11 (2018) 477–502.
[40] K. Busch, M. Kny, N. Huang, et al., Inhibition of the NLRP3/IL-1β axis protects against sepsis-induced cardiomyopathy, J. Cachex-.-. Sarcopenia Muscle 12 (2021) 1653–1668.
[41] Y. Hattori, K. Hattori, T. Suzuki, et al., Recent advances in the pathophysiology and molecular basis of sepsis-associated organ dysfunction: Novel therapeutic implications and challenges, Pharmacol. Ther. 177 (2017) 56–66.
[42] T. Imaizumi, N. Matsuda, K. Tomita, et al., Activator Protein-1 Decoy Oligodeoxynucleotide Transfection Is Beneficial in Reducing Organ Injury and Mortality in Septic Mice, Crit. Care Med. 46 (2018) e435–e442.
[43] S. Imbaby, N. Matsuda, K. Tomita, et al., Beneficial effect of STAT3 decoy oligodeoxynucleotide transfection on organ injury and mortality in mice with cecal ligation and puncture-induced sepsis, Sci. Rep. 10 (2020) 15316.
[44] C. Thiemermann, J. Vane, Inhibition of nitric oxide synthesis reduces the hypotension induced by bacterial lipopolysaccharides in the rat in vivo, Eur. J. Pharmacol. 182 (1990) 591–595.
[45] C. Szabó, J.A. Mitchell, C. Thiemermann, et al., Nitric oxide-mediated hyporeactivity to noradrenaline precedes the induction of nitric oxide synthase in endotoxin shock, Br. J. Pharmacol. 108 (1993) 786–792.
[46] L. Landin, J.A. Lorente, E. Renes, et al., Inhibition of Nitric Oxide Synthesis Improves the Vasoconstrictive Effect of Noradrenaline in Sepsis, Chest 106 (1994) 250–256.
[47] A. Thooft, R. Favory, D. Salgado, et al., Effects of changes in arterial pressure on organ perfusion during septic shock, Crit. Care 15 (2011) R222.
[48] A. Rhodes, L.E. Evans, W. Alhazzani, et al., Surviving Sepsis Campaign: International Guidelines for Management of Sepsis and Septic Shock: 2016, Intensive Care Med. 43 (2017) 304–377.